Localized Soft Mode at Optical-Field-Induced Fréedericksz Transition in a Nematic Liquid Crystal

I. Drevenšek Olenik,[1,2] M. Jazbinšek,[2] and M. Čopič[1,2]
[1]*Jozef Stefan Institute, Jamova 39, 1001 Ljubljana, Slovenia*
[2]*Faculty of Mathematics and Physics, University of Ljubljana, 1000, Ljubljana, Slovenia*
(Received 26 August 1998)

Collective orientational fluctuations near optical-field-induced Fréedericksz transition in a homeotropically aligned nematic liquid crystal 5CB are studied by dynamic light scattering. A softening of the orientational fluctuation mode corresponding to the transverse profile of the optical field was detected. The observed properties of the soft mode are described by a single localized bound mode of the orientational fluctuations in an effective potential well formed by the optical field. The results of the model agree with the experiment without any adjustable parameter. [S0031-9007(99)08655-X]

PACS numbers: 61.30.Gd, 64.70.Md, 78.35.+c

The interaction of a laser beam with liquid crystals exhibits a variety of interesting nonlinear phenomena. A well known and particularly interesting case is the optical Fréedericksz transition (OFT) [1], in which the dielectric torque exerted on the nematic director by the optical field causes an inhomogeneous reorientation of the initially homogeneous structure and thereby changing the effective refractive index produces a system of light fringes [2]. These can be either static or show time dependent oscillatory or even chaotic behavior [3–8]. Fréedericksz transition produced by the static electric field occurs at a well defined threshold that depends on the sample thickness [9]. The same is true for OFT, but the threshold optical field strength E_{tr} also depends on the laser spot size [10,11].

The instability associated with the OFT can be interpreted as the slowing down of some thermal fluctuation mode of the director field which freezes at E_{tr}. In the usual case of homogeneous low frequency external field this soft mode is of a plane wave form with the critical wave vector determined by the sample thickness. The analysis of transmitted light polarization noise and light scattering have shown that in homogeneous fields the relaxation time and the mean square value of the amplitude of the critical fluctuation increase with increasing field as $(E_{\mathrm{tr}}^2 - E^2)^{-1}$ [12–16]. The case of OFT is more complex due to the finite laser spot size which strongly affects the threshold field [10,11]. The previous investigations have focused mostly on the determination of the threshold field and the perturbed director profile [8–11], while the dynamic behavior of the critical fluctuations has to our knowledge not been reported yet.

In this Letter we present the first experimental light scattering evidence of the soft mode in OFT. We show that it can be described as a special mode of the orientational fluctuation spectrum which does not have a plane wave form. The optical field acts on the director as an effective potential well of finite depth, for which the nematic equation of motion has exactly one localized bound solution, analogous to the quantum mechanical problem of a particle in a shallow well or to propagation of light in a single mode optical fiber. The peculiarity of the OFT, which causes the instability, is that the elastic torque transmitted from the walls of the sample acts so as to make the relaxation rate of the soft mode finite while the optical field polarized perpendicularly to the average director drives the relaxation rate towards zero and at the same time makes the soft mode more and more localized. This interplay of competing torques and mode localization makes the dependence of the relaxation rate on the external optical field much more interesting and has novel consequences on the soft mode observation by light scattering.

In our dynamic light scattering (DLS) experiment a homeotropically aligned sample of nematic liquid crystal 4-pentyl-4′-cyanobiphenyl (5CB, Merck Ltd.) was prepared with two silane (DMOAP) covered glass plates. The thickness of the sample L was 120 μm. In a conventional DLS setup two cw laser beams were used simultaneously: the molecular reorientation inducing Ar ion laser beam (pump beam) with waist size $w_0 \approx 20$ μm and a weak He-Ne laser beam (probe beam) with $w_0' \approx 15$ μm (Fig. 1).

All the measurements were performed at room temperature of 24 °C. The autocorrelation function $g^{(2)}(t) = \langle I_s(t')I_s(t' + t)\rangle$ of the scattered light intensity I_s of definite polarization and propagation direction was recorded by a digital autocorrelator. The detection of either the pump or the probe beam light scattering was selected by use of an appropriate optical interference filter mounted in front of the detector.

The threshold power P_{tr} was found to be 40 mW. If $w_0 \gg L$, the induced director reorientation would be as in the plane wave situation and the magnitude of the critical optical field E_c would be determined by

$$\frac{1}{2}\,\frac{\varepsilon_\perp}{\varepsilon_\parallel}\,\varepsilon_0\varepsilon_a E_c^2 = K\left(\frac{\pi}{L}\right)^2, \tag{1}$$

where $\varepsilon_\parallel$ and $\varepsilon_\perp$ are the components of the optical dielectric tensor along and perpendicularly to the nematic director $\mathbf{n}$, $\varepsilon_a = \varepsilon_\parallel - \varepsilon_\perp$ is optical anisotropy, and K is the

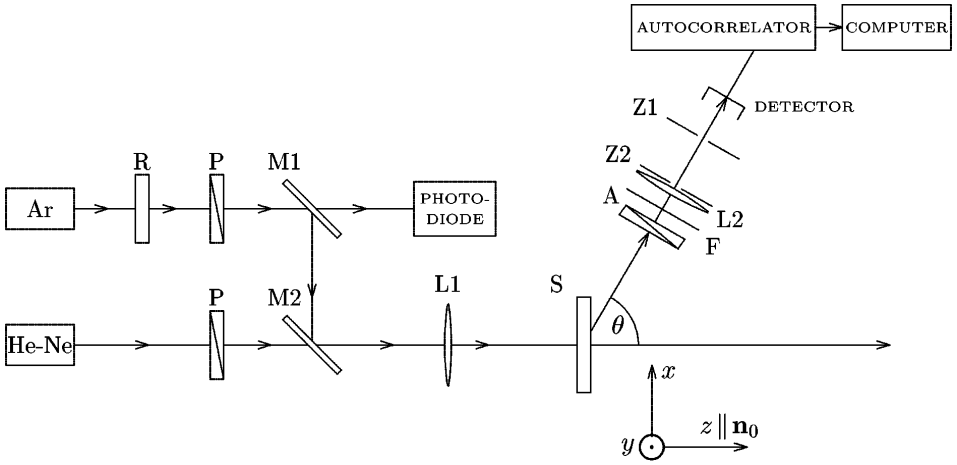

FIG. 1. Experimental setup with polarization rotator R, polarizers P; analyzer A; lenses L1, L2; pinholes Z1, Z2; dicroic mirrors M1, M2; color filter F; Ar laser beam (pump beam) with $\lambda = 514.5$ nm; He-Ne laser beam (probe beam) with $\lambda = 632.8$ nm; and sample S.

average Frank elastic constant. Taking into account the values of these material parameters for 5CB as reported in the literature [6,17], expression (1) gives for the corresponding laser power $P_c \approx 3$ mW. The about 13 times larger value of P_{tr} observed in our experiment shows the importance of the finite beam size and is in agreement with other results obtained at the similar ratio of L/w_0 [10,11].

The measurements were performed at a scattering angle θ of 0.7°. The pump beam as well as the probe beam propagated in the direction normal to the sample walls, i.e., along the z axis, and were linearly polarized along the x axis (Fig. 1). The polarization of the scattered light was selected to be within the scattering plane, that is, in the xz plane. In homeotropic alignment such a geometry probes solely the bend-splay fluctuations [9]. The components of the corresponding scattering wave vector are $q_x = 14.9 \times 10^4\ \mathrm{m}^{-1}$ and $q_z = 4.7 \times 10^2\ \mathrm{m}^{-1}$ for the pump beam and $q_x = 12.4 \times 10^4\ \mathrm{m}^{-1}$ and $q_z = 3.8 \times 10^2\ \mathrm{m}^{-1}$ for the probe beam, while for comparison $\pi/w_0 = 15.7 \times 10^4\ \mathrm{m}^{-1}$. Because of the small scattering angle and nearly parallel in- and outgoing polarizations a lot of elastic scattering made the regime of the detection entirely heterodyne; the inelastic scattering contributed only about 1% of the total scattered power. For the incident optical power below the threshold value P_{tr} the time dependence of the measured autocorrelation function $g^{(2)}(t)$ was reasonably well fitted to a single exponential decay.

The dependence of the inverse relaxation time $1/\tau$ of the fluctuations as a function of the incident optical power P as obtained from the DLS of the pump beam and the DLS of the probe beam is shown in Fig. 2. From $P = 0$ to $P \sim 0.7P_{\mathrm{tr}}$ the inverse relaxation time is approximately constant. At about $0.7P_{\mathrm{tr}}$ the behavior changes significantly; the value of $1/\tau$ starts to decrease with increasing P and goes to zero at P_{tr}.

The obtained results can be explained in the following way. To find the spatial profile of the normal modes and evaluate their relaxation times one has to solve the Euler-Lagrange-Rayleigh dynamic equation for small director fluctuations in an optical field of Gaussian shape [8]. The simplest level of this procedure is to apply the one-constant approximation and neglect the backflow effects, as well as optically induced temperature and density changes. With these approximations and assuming strong anchoring at sample surfaces, i.e., $\delta\mathbf{n}(t, z = 0, L) = 0$, the dynamic equation for the x component of the fluctuations described as $\delta\mathbf{n} = (\xi_x, \xi_y, 0)$ is [8]

$$\Delta\xi_x + \frac{1}{2}\,\varepsilon_0\varepsilon_a\,\frac{\varepsilon_\perp}{\varepsilon_\parallel}\,\frac{1}{K}\,|E(x,y)|^2\xi_x = \frac{\eta}{K}\,\frac{\partial\xi_x}{\partial t}\,, \qquad (2)$$

where $E(x,y) = E_0 e^{-(x^2+y^2)/w_0^2}$ is the amplitude of the optical field, and η is the effective viscosity of the material. The fluctuations ξ_y in a direction perpendicular to the field remain unaffected and have the form of plane waves.

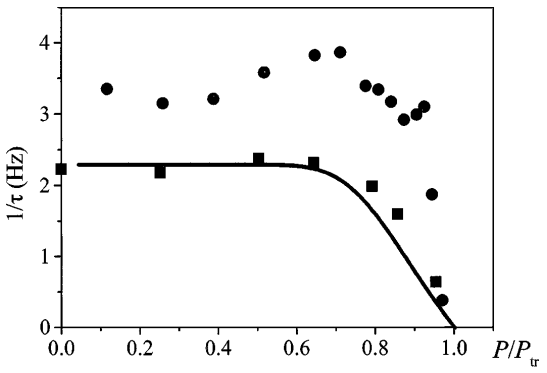

FIG. 2. The dependencies of the inverse relaxation time of the bend-splay fluctuations on the incident optical power of the pump wave. The circles correspond to the pump beam scattering; the squares correspond to the probe beam scattering. The values for pump and probe beam differ due to different magnitudes of the scattering wave vector. The solid line is a plot of Eq. (7).

To facilitate the analysis we approximate the Gaussian beam shape with a simple form [8,10]

$$|E(x,y)| \approx \begin{cases} E_0, & \rho < \frac{1}{\sqrt{2}}\, w_0\,, \\ 0, & \rho > \frac{1}{\sqrt{2}}\, w_0\,, \end{cases} \tag{3}$$

where $\rho = \sqrt{x^2 + y^2}$. With this approximation the resulting equation for ξ_x expressed in cylindrical coordinates as $\xi_x = \xi_0 f(\rho,\varphi)\sin(n\frac{\pi}{L}z)e^{-t/\tau}$ becomes

$$-\frac{\partial^2 f}{\partial \rho^2} - \frac{1}{\rho}\frac{\partial f}{\partial \rho} - \frac{1}{\rho^2}\frac{\partial^2 f}{\partial \varphi^2} - \left(\frac{E_0^2}{E_c^2}\frac{\pi^2}{L^2} - n^2\frac{\pi^2}{L^2}\right) f = \frac{\eta}{K\tau} f \tag{4}$$

with E_c defined in Eq. (1). Equation (4) is analogous to the Schrödinger equation for a two-dimensional cylindrical potential well.

The relaxation rate of the fluctuations is given by the eigenvalues of Eq. (4) with the boundary conditions that $f(\rho,\varphi)$ and $\partial f(\rho,\varphi)/\partial\rho$ are both continuous at $\rho = w_0/\sqrt{2}$. In our experiment the scattering vector was nearly perpendicular to the z axis, so that $q_z \ll \pi/L$ and only the modes with $n = 1$ contributed to the observed scattered field. For $n = 1$ there is exactly one discrete eigenvalue corresponding to the only bound state in the case of a particle in a shallow well. The other eigenvalues belong to the continuous spectrum and correspond to the usual director fluctuations which extend over the whole sample and have the form of plane waves which are slightly perturbed in the vicinity of the laser spot. The bound mode is localized and extends to a distance $1/\kappa$ from the well boundary, where $\kappa^2 = \eta/K\tau - \pi^2/L^2$. Setting $\upsilon^2 = (\pi w_0/\sqrt{2}\,L)^2(E_0^2/E_c^2 - 1) + \eta w_0^2/(2K\tau)$ and $s = \kappa w_0/\sqrt{2}$, the boundary conditions yield

$$\upsilon\frac{J_0'(\upsilon)}{J_0(\upsilon)} = s\frac{K_0'(s)}{K_0(s)}\,, \tag{5}$$

where J_0 is the Bessel and K_0 the Kelvin function.

From Eq. (5) one can numerically find υ and s. The relaxation rate is then given by

$$\frac{1}{\tau} = \frac{K}{\eta}\frac{\pi^2}{L^2}[1 - s^2/p^2], \tag{6}$$

where $p = \pi w_0/\sqrt{2}\,L$. The resulting inverse relaxation time $1/\tau$ for the bound mode as a function of incident power $P/P_c \propto p^2E_0^2/E_c^2$ is shown in Fig. 3a. The behavior of this mode is crucial for the appearance of the OFT. It is bound at any value of the incident optical power P. The relaxation rate $1/\tau$ is nearly constant to about 70% of the threshold power and then starts to decrease significantly, going to zero at $s = p$, where the OFT occurs. For our experimental situation $p = 0.37$ and the threshold should be reached at $P/P_c = 10.1$, what is about 20% below the experimentally observed value.

The spatial extension of the bound mode is $1/\kappa = \rho_0 = w_0/\sqrt{2}\,s$ and is shown in Fig. 3b. The value of ρ_0, which is infinite at the beginning, rapidly decreases with increasing power and reaches the value of around $3w_0$ at threshold. The decrease of ρ_0 explains the specific behavior of the inverse relaxation time. The increasing incident optical power and the associated destabilizing action of the optical field tend to decrease the value of $1/\tau$, while at the same time the corresponding decrease of the transverse size of the mode and related increase of the elastic energy act in the opposite way. Because of the competition of these two effects the resulting value of $1/\tau$ is almost constant at low powers and starts to decrease significantly only in the vicinity of the threshold, when the first effect becomes predominant. The mean square amplitude of the critical mode is proportional to the relaxation time of the mode τ [12] and therefore rapidly increases above around $0.7P_{\rm tr}$, resulting in a prominent increase of the inelastic light scattering at low scattering angles, which can be easily noticed in the experiment as an increased twinkling of the outgoing laser beam.

The dependence of the size of the bound mode on P has important consequences for the observed scattered light intensity correlation function. At any laser power, both the free modes of the continuous part of the eigenvalue spectrum of Eq. (2) and the bound mode contribute to light scattering at selected scattering wave vector **q**. The contribution of each free mode is proportional to V_s^2, where $V_s = \pi w_0^2 L$ is the scattering volume, while the number of the contributing modes is proportional to $1/V_s$ due to the increased volume of the wave-vector space for $q \sim w_0$. So the free-mode contribution to the total scattering intensity is given by $I_q = A\varepsilon_a^2 kT\eta\tau_q\pi w_0^2 L$, where A is a constant containing the details of the scattering geometry. The free-mode relaxation time is given by

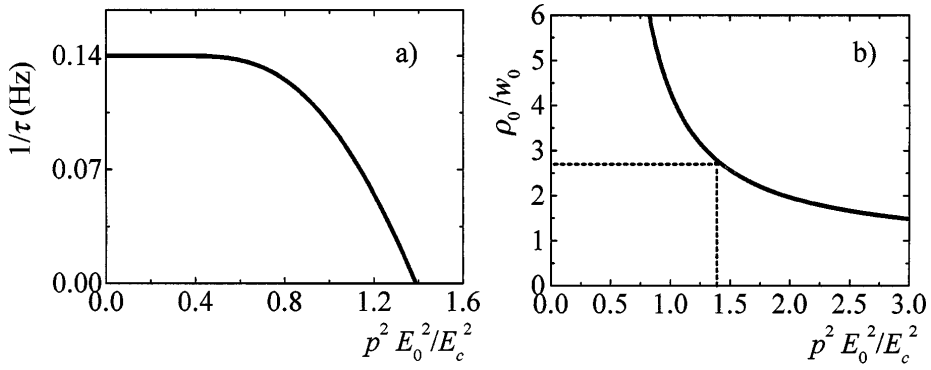

FIG. 3. (a) The dependence of the inverse relaxation time of the bend-splay fluctuations on the relative incident optical power $(E_0/E_c)^2$. The scaling factor on the x axis is $p = \pi w_0/L\sqrt{2} = 0.37$. (b) The dependence of the characteristic size of the transverse profile of the critical mode on the relative incident optical power $(E_0/E_c)^2$. The vertical dashed line designates the threshold of the OFT.

$\tau_q = (\eta/K)q^2$, where q is the magnitude of the scattering vector. By the equipartition theorem, the mean square of the bound mode amplitude ξ_0 is inversely proportional to the volume of the mode, $\langle \xi_0^2 \rangle \propto kT\eta\tau_0/L\rho_0^2$, so that the bound mode scattering intensity is $I_0 = A\varepsilon_a^2 \langle \xi_0^2 \rangle V_s^2 = A\varepsilon_a^2 kT\eta\tau_0 \pi w_0^2 L(w_0\kappa)^2$. This result can be interpreted in an intuitively obvious way that the bound-mode contribution is proportional to the ratio of the illuminated area to the total mode area. The increase in the inelastic scattering related to the squeezing of the bound-mode area is well evident in Fig. 4, which shows the dependence of the ratio of inelastic to elastic light scattering intensity ($I_{\mathrm{inel}}/I_{\mathrm{el}}$) on the incident optical power P for the case of pump beam scattering. The data were obtained from the corresponding heterodyne autocorrelation function $g^{(2)}(t)$ as $I_{\mathrm{inel}}/I_{\mathrm{el}} = \frac{1}{2}\{[g^{(2)}(t=0)/g^{(2)}(t=\infty)] - 1\}$. Similarly to the dependence of $1/\tau$, $I_{\mathrm{inel}}/I_{\mathrm{el}}$ starts to change at about $0.7P_{\mathrm{tr}}$ and then grows until the threshold is reached. The total scattered intensity I_{tot}, which originates predominantly from elastic scattering background shows no significant changes in the whole interval from $0 < P < P_{\mathrm{tr}}$ but increases linearly with increasing incident power. This justifies that the observed increase in the value of $I_{\mathrm{inel}}/I_{\mathrm{el}}$ is due to the increase of the inelastic light scattering and not due to some changes in the elastic scattering background.

The observed relaxation rate $1/\tau_{\mathrm{obs}}$ is the average of the $1/\tau_q$ and $1/\tau_0$ weighted by the respective scattering intensities and can be expressed as

$$\frac{1}{\tau_{\mathrm{obs}}} = \frac{1 + \kappa^2 w_0^2}{\tau_q + \kappa^2 w_0^2 \tau_0}. \qquad (7)$$

At small P, κ is very small, and $1/\tau_{\mathrm{obs}} \simeq 1/\tau_q$, while close to OFT, the $\kappa w_0 \simeq 1/3$, and $\tau_0 \gg \tau_q$, so $1/\tau_{\mathrm{obs}}$ decreases to a value close to $10/\tau_0$.

All the parameters needed to evaluate expression (7) are known. From the known values of K/η [18], we get $1/\tau_q = 2\ \mathrm{s}^{-1}$ at small P. Expression (7) is plotted in Fig. 2 as a solid line, and the agreement with the measured values is quite good, since there are no free parameters in the model.

To conclude, we have experimentally observed the critical slowing down of the director fluctuations in the vicinity of the optical field induced Fréedericksz transition in a homeotropic nematic liquid crystal cell. The critical mode has the unusual property that it is localized by the optical field. The observed dependence of the relaxation rate of the critical mode on the input optical power is very different from the linearly decreasing behavior, which is characteristic for the Fréedericksz transition in homogeneous external fields. The observed properties of the critical mode are well described by the simple model of the director dynamics in a square well effective potential formed by the optical beam.

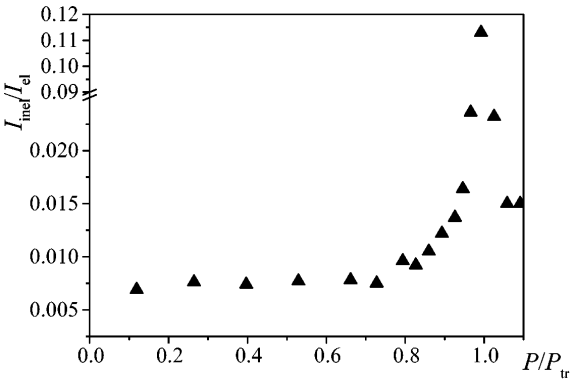

FIG. 4. The dependence of the inelastic light scattering intensity of the pump wave on the incident optical power.

This work was supported by Ministry of Science and Technology of Slovenia (Grant No. J1-7474) and European Union (Grant No. IC15-CT96-0744).

[1] S. D. Durbin, S. M. Arakelian, and Y. R. Shen, Phys. Rev. Lett. **47**, 1411 (1981).
[2] J. J. Wu, S.-H. Chen, J. Y. Fan, and G. S. Ong, J. Opt. Soc. Am. B **7**, 1147 (1990).
[3] E. Santamato, B. Daino, M. Romagnoli, M. Settembre, and Y. R. Shen, Phys. Rev. Lett. **57**, 2423 (1986).
[4] H. L. Ong, Phys. Rev. A **28**, 2393 (1983).
[5] E. Santamato, G. Abbate, P. Maddalena, and Y. R. Shen, Phys. Rev. A **36**, 2389 (1987).
[6] E. Santamato, G. Abbate, P. Maddalena, L. Marruci, and Y. R. Shen, Phys. Rev. Lett. **64**, 1377 (1990).
[7] G. Cipparrone, V. Carbone, C. Versace, C. Umeton, and R. Bartolino, Phys. Rev. E **47**, 3741 (1993).
[8] N. V. Tabiryan, A. V. Sukhov, and B. Ya. Zeldovich, Mol. Cryst. Liq. Cryst. **136**, 1 (1986) (p. 86, and references therein).
[9] See, for instance, P. G. De Gennes, *The Physics of Liquid Crystals* (Clarendon, Oxford, 1974).
[10] L. Csillag, I. Janossy, V. F. Kitaeva, N. Kroo, and N. N. Sobolev, Mol. Cryst. Liq. Cryst. **84**, 125 (1982).
[11] I. C. Khoo, T. H. Liu, and P. Y. Yan, J. Opt. Soc. Am. B **4**, 115 (1987).
[12] P. Galatola, C. Oldano, and M. Rajteri, Phys. Rev. E **49**, 1458 (1994).
[13] S. M. Arakelyan, L. E. Arushanyan, and Yu. S. Chilingaryan, Zh. Tekh. Fiz. **56**, 1949 (1986).
[14] K. Eidner, M. Lewis, H. K. M. Vithana, and D. L. Johnson, Phys. Rev. A **40**, 6388 (1989).
[15] P. Allia, P. Galatola, C. Oldano, P. Taverna Valabrega, L. Trossi, and C. Aprato, Mol. Cryst. Liq. Cryst. **225**, 23 (1993).
[16] P. Galatola and M. Rajteri, Phys. Rev. E **49**, 623 (1994).
[17] M. S. Sefton, A. R. Bowdler, and H. J. Coles, Mol. Cryst. Liq. Cryst. **129**, 1 (1985).
[18] G. Chen, H. Takezoe, and A. Fukuda, Liq. Cryst. **5**, 341 (1989).